Phase transition in the $Zr_{1-x}Sc_xB_{12}$ system

K. Hamada, M. Wakata, N. Sugii, K. Matsuura, K. Kubo, and H. Yamauchi
Superconductivity Research Laboratory, International Superconductivity Technology Center, 10-13 Shinonome 1-chome, Koto-ku, Tokyo 135, Japan
(Received 7 April 1993)

A metal-metal transition followed by a structural transition near room temperature was found in the solid solutions between cubic ZrB_{12} and tetragonal ScB_{12}, i.e., in $Zr_{1-x}Sc_xB_{12}$ with compositions in the range of $0.1 \leq x \leq 0.9$. The high-temperature phase had a face-centered-cubic (fcc) structure with a lattice parameter of $a_0 \sim 7.4$ Å and n-type carriers. The low-temperature phase had a period twice longer than for the fcc lattice in the direction of [111], the trigonal space group of $R\bar{3}m$ and p-type carriers. This phase transition was of first order and was thought to be caused by the Jahn-Teller effect based on the deformation of B_{12} clusters followed by the displacement of metallic atoms.

I. INTRODUCTION

Since the discovery of high-temperature superconductivity,[1] great efforts have been devoted to obtain new superconductors. The mechanism of high-temperature superconductivity has not been understood, but it is accepted that strongly correlated electrons in the CuO_2 plane are important for high-temperature superconductivity. In fact, a variety of layered cuprates were discovered and most of them showed superconductivity when an adequate amount of carriers were introduced in the CuO_2 planes.

Various kinds of layered structural oxides not containing Cu have also been synthesized. It is useful to compare crystallographic and electronic structures of these materials with those of layered cuprates. Among oxides containing no Cu, superconductivity of T_c (critical temperature) ~ 30 K was reported in the Ba-K-Bi-O system.[2] The superconductor did not have a layered structure and has not been included in the category of high-temperature superconductors, though the T_c exceeded those for conventional low-temperature superconductors.

The search for new superconductors has been conducted not only among inorganic nonoxide materials but also among organic materials. Superconductivity in the potassium metal-doped fullerrene C_{60} was a stimulative discovery.[3] The structure of this superconductor is either a face-centered-cubic or a hexagonal close-packed structure of C_{60} clusters, where the metal atoms are located in the interstitial openings. Although it is thought that the superconductivity is understood by BCS theory based on an ordinary band picture, the T_c was surprisingly increased with increasing the ionic radius of the alkali metal as a dopant, and reached 33 K.[4]

It is known that boron atoms form clusters as carbon atoms do. However, such clusters do not exist as molecules but in solid crystals such as octahedral B_6 clusters in MB_6 (M=Ca, Sr, Ba, La, Ce, Gd, Tb, Th, and U), icosahedral B_{12} clusters in α-rhombohedral boron, $B_{12}P_2$ and $B_{12}As_2$, and so on. Intermetallic compounds, MB_{12} (M=U, Zr, Y, and Sc), include cubo-octahedral B_{12} clusters, which are different from icosahedra. In MB_{12}, the metallic atoms, M, are located in interstitial openings among the close-packed B_{12} clusters. Among these compounds, both ZrB_{12} and ScB_{12} are superconductors with the critical temperatures of 6.03 and 0.39 K, respectively.[5]

The electronic structures are quite different between MB_{12} and M'_3C_{60} (M'=alkaline metal), in spite of the similarity in the crystal structure. A C_{60} cluster has the electronic structure of a closed-shell configuration, but a B_{12} cluster requires two additional electrons to achieve it.[6] Therefore, it is interesting to study the difference in the superconducting properties of the boron-cluster compounds and the carbon-cluster compounds.

In this work, we synthesized solid solutions of the two compounds, ZrB_{12} and ScB_{12}, i.e., $Zr_{1-x}Sc_xB_{12}$, and studied their structural and physical properties.

II. EXPERIMENT

The $Zr_{1-x}Sc_xB_{12}$ samples were prepared by solid-state reaction method using ZrO_2 (purity: 98%), Sc_2O_3 (99.9%), and B (97%) powders. The deoxidization was performed by adding excess B powder following the reaction formula:

$$(1-x)ZrO_2+(x/2)Sc_2O_3+(14-x/2)B \rightarrow Zr_{1-x}Sc_xB_{12}+(2-x/2)BO\uparrow . \quad (1)$$

The Sc contents x were 0, 0.05, 0.1, 0.15, 0.2, 0.25, 0.3, 0.4, 0.5, 0.6, 0.7, 0.8, 0.9, and 1.0. The powder mixture was pressed into pellets and sintered at 1820 °C for 1 h in a vacuum (10^{-5} Torr before heating) furnace with carbon heaters.

The phase identification and structural analysis were made by x-ray powder diffraction (XRD) using Cu $K\alpha$ radiation and electron diffraction (ED). The homogenei-

0163-1829/93/48(10)/6892(7)/$06.00

ty of the samples was examined by electron probe microanalysis (EPMA). The temperature dependence of electrical resistivity was measured by a four-probe technique. The temperature dependence of the magnetic susceptibility was measured by a superconducting quantum interference device magnetometer in a magnetic field of 1 T for the samples with $x=0$, 0.15, and 1.0. For these samples, the thermoelectric power was also measured in the temperature range from 50 to 310 K. In this measurement a temperature gradient of 0.3 K was applied over the sample length of 5–10 mm.

III. RESULTS

A. Physical properties

The temperature dependence of electrical resistivity is shown in Fig. 1(a) for the samples with $x=0$, 0.05, 0.1, 0.15, 0.2, 0.25, and 0.3. The samples with $x \leq 0.1$ showed superconductivity with the critical temperatures (T_c^S) of ~ 6 K. The resistivity increased monotonically with increasing x. For the samples with the compositions in the range of $0.1 \leq x \leq 0.3$, anomalous behaviors were clearly seen in the temperature dependence of resistivity. For the sample with $x=0.1$, a plateau was seen around 100 K. For the sample with $x=0.15$, the resistivity decreased with decreasing temperature down to ~ 180 K. Below this temperature it increased abruptly with decreasing temperature. However, it began to decrease again below ~ 80 K, although the temperature dependence was quite small. In the temperature range of ~ 80 K $< T < \sim 200$ K, there existed a hysteresis in the temperature dependence of resistivity, i.e., the resistivity was higher when temperature increased than when it decreased. This anomaly appears due to a phase transition of the first order, that is, a metal-metal transition with a wide transition region. The critical temperature of this phase transition (T_c^M) apparently increased monotonically with increasing x with a rate of $\Delta T_c^M/\Delta x \sim 10^3$ K.

Figure 1(b) shows the temperature dependence of resistivity for the samples with $x=0.4$, 0.5, 0.6, 0.7, 0.8, 0.9, and 1.0. No anomalies were observed. However, slight temperature dependences of resistivity for the samples with $x=0.4$ and 0.5 were parallel to those for the samples with $x=0.15$, 0.2, 0.25, and 0.3 in the low-temperature region. Therefore, it was estimated that T_c^M was higher than 300 K for these two samples. It was also consistent with the result shown in Fig. 1(a), that electrical resistivity increased with increasing x. However, a further increase in x lowered resistivity at low temperatures and made the temperature dependence deeper. Figure 2 shows the temperature dependence of the dc susceptibility (χ) for the samples with $x=0$, 0.15, and 1.0. For both samples with $x=0$ and 1.0, χ was almost independent of temperature and showed diamagnetism. The absolute value of χ of ScB_{12} was three times higher than that for ZrB_{12}. This suggested that the diamagnetism stemmed from Sc^{3+} and Zr^{4+} ions. On the other hand, the diamagnetism for the sample with $x=0.15$ was enhanced in the transition region more than 20%. This also suggested that the electronic structure was changed drastically due to the phase transition. It was not clear if a hysteresis existed in the χ vs temperature curves. The increase of χ at low temperatures was thought to be due to the existence of the paramagnetic impurities.

In order to investigate the nature of charge carriers, thermoelectric power was measured in the temperature range from 50 to 310 K for the samples with $x=0$, 0.15, and 1.0. As shown in Fig. 3, the Seebeck coefficient was negative for ZrB_{12} and positive for ScB_{12}. On the other hand, for the sample with $x=0.15$, it was negative at high temperatures but abruptly changed its sign in the transition range. At temperatures higher than T_c^M, the sample was an n-type metal, as is ZrB_{12}, and had a carrier

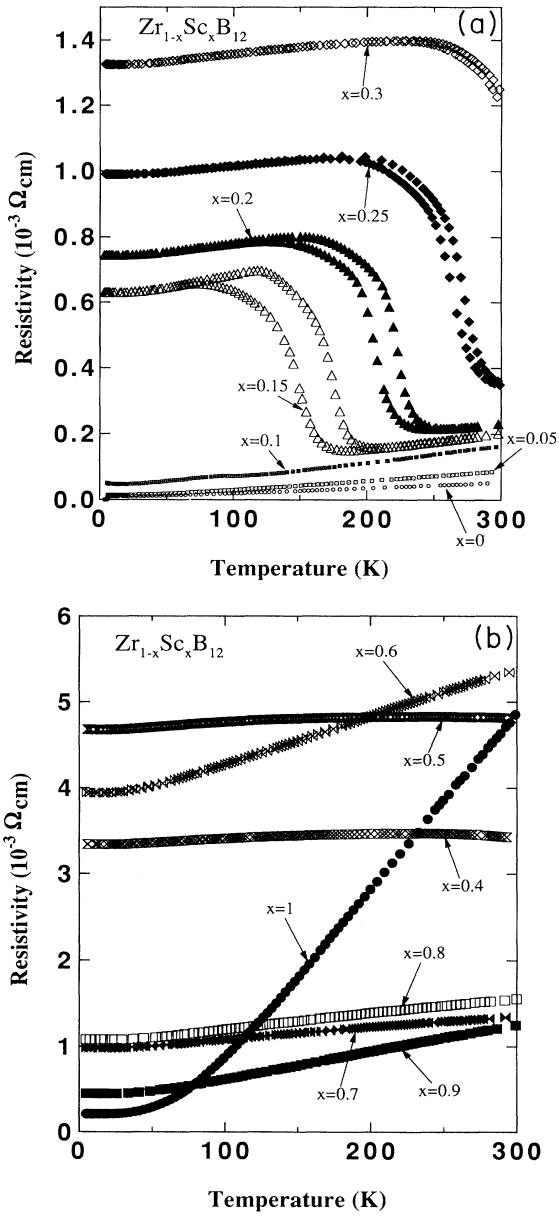

FIG. 1. The temperature dependence of the electrical resistivity for the samples of $Zr_{1-x}Sc_xB_{12}$ [$x=0$, 0.05, 0.1, 0.15, 0.2, 0.25, and 0.3 (a) and 0.4, 0.5, 0.6, 0.7, 0.8, 0.9, and 1.0 (b)].

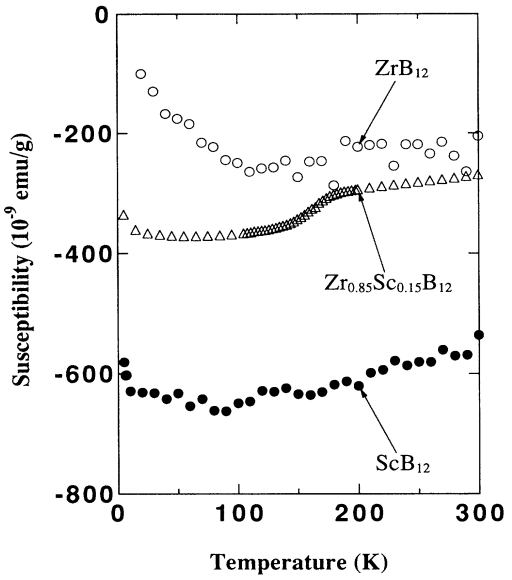

FIG. 2. The temperature dependence of the dc susceptibility for the samples of $Zr_{1-x}Sc_xB_{12}$ with $x=0$, 0.15, and 1.0.

density lower than ZrB_{12}. At temperatures lower than T_c^M, it was a p-type metal, as is ScB_{12}, and had a carrier density lower than ScB_{12}.

B. Structure

Figure 4 shows XRD patterns taken at room temperature for the samples with $x=0$, 0.1, 0.2, 0.3, 0.4, 0.5, 0.6, 0.7, 0.8, 0.9, and 1.0. Except for ScB_{12}, which had a tetragonal structure with the lattice parameters of $a=5.22$ Å and $c=7.35$ Å, the main peaks of the samples with $x \geq 0.1$ were successfully indexed for the face-centered-cubic (fcc) structure with the lattice parameter of $a \equiv a_0 \sim 7.4$ Å. As marked with crosses in Fig. 4, a small amount of impurity phase coexisted. This phase was found to be ZrB_2 by EPMA and XRD. For the samples with $0.3 \leq x \leq 0.9$, other weak peaks marked with open circles appeared. The intensity of such peaks is maximum for x at ~ 0.5. It was made clear from Fig. 5 that these peaks did not correspond to any impurity phases but to a different phase that appeared due to the structural transition.

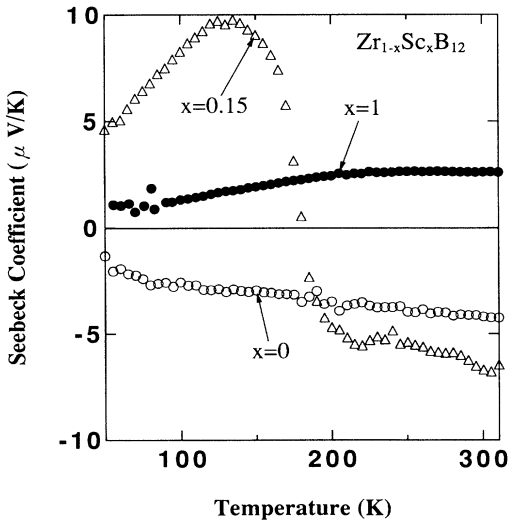

FIG. 3. The temperature dependence of the Seebeck coefficient for the samples of $Zr_{1-x}Sc_xB_{12}$ with $x=0$, 0.15, and 1.0.

The temperature dependence of the XRD pattern for the sample with $x=0.15$ is shown in Fig. 5. The pattern, which showed the existence of fcc $Zr_{1-x}Sc_xB_{12}$ and a small amount of ZrB_2, remained unchanged from room temperature down to 190 K. The aforementioned peaks appeared below 180 K, which was close to T_c^M. All the peaks increased in their intensity with decreasing temperature down to 100 K, which was near the lowest temperature of the transition region, and leveled off at low temperatures. Therefore, at the same time when the metal-metal transition was detected from the temperature dependence of resistivity, a structural transformation occurred.

Figure 6 shows an electron-diffraction pattern taken at room temperature for the sample with $x=0.3$. The direction of electron beam was along the [110] direction in the cubic reciprocal-lattice space. It was found that some extra spots appeared at the center of all nearest-neighbor spots along the [111] direction. This means that the lattice dimension at low temperatures is twice larger than that at high temperatures in a certain direction.

IV. DISCUSSIONS

A. Structure

Figure 7 shows the crystal structures of ZrB_{12} and ScB_{12}. Both borides have a NaCl-type structure consisting of Zr or Sc atoms and cubo-octahedral B_{12} clusters. ZrB_{12} has an fcc structure with the lattice parameter of $a=7.408$ Å and the space group of $Fm3m$ as shown in Fig. 7(a).[7] On the other hand, ScB_{12} has a tetragonal structure with the lattice parameters of $a=5.22$ Å and $c=7.35$ Å and the space group of $I4/mmm$ as shown in Fig. 7(b).[8] This structure has not been exactly determined, but appears to be a distorted ZrB_{12} structure. The structure of $Zr_{1-x}Sc_xB_{12}$ at high temperatures is thought to be identical with that of ZrB_{12}. Then, what is the structure of low temperatures?

As shown in Fig. 5, all the peaks in the XRD at high temperatures remain down to low temperatures. All the peaks which appeared at low temperatures were weak. This fact suggests that the structural change from one at high temperatures to another at low temperatures is not so drastic but the crystal symmetry is a little lowered. The square of the ratio between the lattice parameter of the fcc structure a_0 and the interplanar distance d was an integer plus $\frac{1}{4}$ or $\frac{3}{4}$ for each peak. This fact suggests that to assume a cubic lattice with the lattice parameter of $2a_0$ is a reasonable starting for the determination of crystal

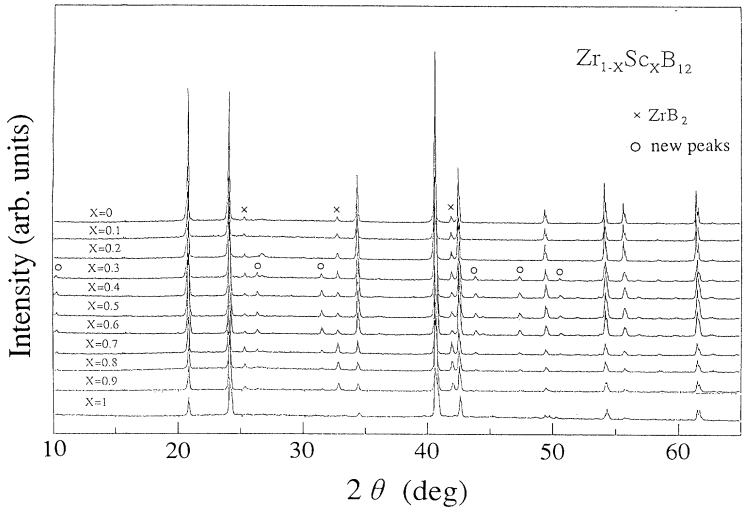

FIG. 4. The XRD patterns at room temperature for the samples of $Zr_{1-x}Sc_xB_{12}$ with $x=0$, 0.1, 0.2, 0.3, 0.4, 0.5, 0.6, 0.7, 0.8, 0.9, and 1.0.

structure. An ED observation as shown in Fig. 6 also supports this assumption.

Based upon the assumed cubic lattice, the Miller indices for peaks existing at high temperatures become twice larger. It was found that the indices for all the peaks were odd numbers. Therefore, the reflection condition is given by

$$(h,k,l=\text{odd})$$

or (2)

$$(h,k,l=\text{even and } h+k,k+l,l+h=4n)\ ,$$

where n is an integer. Condition (2) means that the structure is fcc but has a higher symmetry. In a unit cell of the extended fcc lattice (whose lattice parameter is equal to $2a_0$), the (Zr, Sc) site can be divided into eight groups, each of which can accommodate four (Zr, Sc) atoms. Employing the following basic vectors for the direct space of the fcc lattice at high temperature,

$$\mathbf{a}_0=(0,a_0/2,a_0/2),\quad \mathbf{b}_0=(a_0/2,0,a_0/2)\ ,$$
$$\mathbf{c}_0=(a_0/2,a_0/2,0)\ , \tag{3}$$

the positions of members of each equivalent-site group may be given by

$$\mathbf{r}=n_1\mathbf{a}_0+n_2\mathbf{b}_0+n_3\mathbf{c}_0\ , \tag{4}$$

in which (n_1,n_2,n_3) is for one of the eight different combination of three integers such as (e,e,e), (e,e,o), (e,o,e), etc., where e and o stand for an even and an odd number, respectively. If two or four different groups that are represented by different kinds of (n_1,n_2,n_3) are combined, we can obtain, respectively, four or two extended groups, each of which has a symmetry higher than that of the fcc lattice. Among all the extended groups, the structure shown in Fig. 8, in which the equivalent sites denoted by closed (open) circles satisfies the condition that all or one of n_1, n_2, and n_3 are even (odd) numbers, have the same reflection condition as (2). In this structure, the basic vectors of the direct space $(\mathbf{a},\mathbf{b},\mathbf{c})$ and of the reciprocal-lattice space $(\mathbf{a}^*,\mathbf{b}^*,\mathbf{c}^*)$ are given by

$$\mathbf{a}=\mathbf{c}_0-\mathbf{b}_0,\quad \mathbf{b}=\mathbf{a}_0-\mathbf{c}_0,\quad \mathbf{c}=2\mathbf{c}_0\ ;$$
$$\mathbf{a}^*=-\mathbf{b}_0^*,\quad \mathbf{b}^*=\mathbf{a}_0^*,\quad \mathbf{c}^*=(\mathbf{a}_0^*+\mathbf{b}_0^*+\mathbf{c}_0^*)/2\ , \tag{5}$$

where $\mathbf{a}_0^*=(-1/a_0,\ 1/a_0,1/a_0)$, $\mathbf{b}_0^*=(1/a_0,-1/a_0,\ 1/a_0)$, $\mathbf{c}_0^*=(1/a_0 1/a_0,-1/a_0)$ are the basic reciprocal vectors for the fcc structure at high temperatures. As the set of $\mathbf{c}_0-\mathbf{b}_0$, $\mathbf{a}_0-\mathbf{c}_0$, and $\mathbf{c}_0$ (the set of $-\mathbf{b}_0^*$, $\mathbf{a}_0^*$, and $\mathbf{a}_0^*+\mathbf{b}_0^*+\mathbf{c}_0^*$) is another choice for the basic vectors of the direct (the reciprocal-lattice) space for the fcc structure, the structure at low temperatures should have a period of twice longer than that at high temperatures in the direction of $\mathbf{c}_0$.

Now, there are no space groups for the cubic structure to satisfy the condition (2). If the fcc lattice is transformed into a hexagonal lattice with the basic vectors of $\mathbf{c}_0-\mathbf{b}_0$, $\mathbf{a}_0-\mathbf{c}_0$, and $2(\mathbf{a}_0+\mathbf{b}_0+\mathbf{c}_0)$, as shown in Fig. 8, new Miller indices, (H,K,L) satisfy the reflection condition

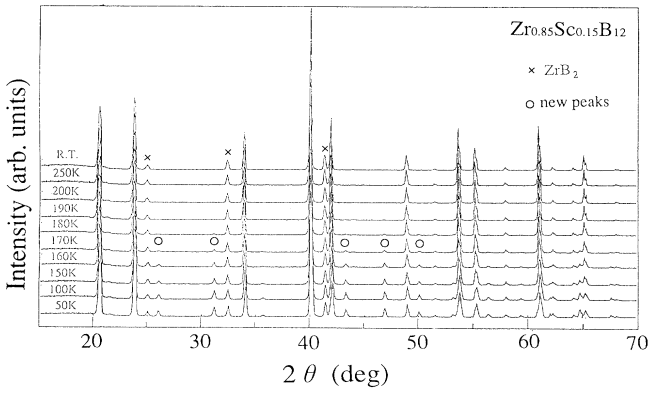

FIG. 5. The XRD patterns at low temperatures for the sample of $Zr_{0.85}Sc_{0.15}B_{12}$.

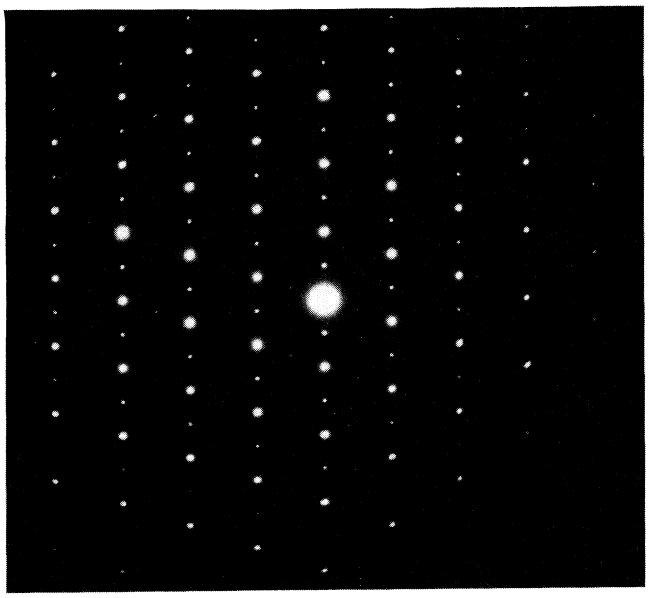

FIG. 6. The electron-diffraction pattern at room temperature for the sample of $Zr_{0.7}Sc_{0.3}B_{12}$.

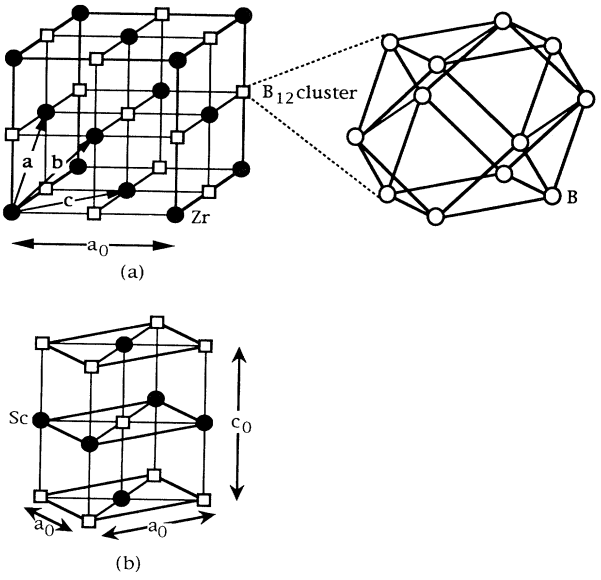

FIG. 7. The lattice structures of ZrB_{12} (a) and ScB_{12} (b).

$$-H+K+L=3n\ , \tag{2'}$$

which coincides with that for the structures of the space groups $R3$, $R\bar{3}$, $R32$, $R3m$, and $R\bar{3}m$. The correspondence between the both Miller indices is given in Table I.

The result of ED shown in Fig. 6 is consistent with our discussion on the XRD data. All the strong spots in Fig. 6 correspond to the Miller indices for the fcc lattice as shown in Fig. 9(a). All the spots including the weak spots were found to be indexed for a hexagonal lattice as shown in Fig. 9(b).

In order to refine the crystal structure, Rietveld analysis was performed for the sample with $x=0.4$. Both analyses based on the space groups $R3m$ and $R\bar{3}m$ gave almost the same results as shown in Table II. As $R\bar{3}m$ has the symmetry higher than $R3m$, it can be concluded that the hexagonal structure has the former space group. It was found that the neighboring metal sites displaced in an opposite direction along the c axis of the hexagonal lattice. On the other hand, it could not be determined whether there existed any distortion of boron clusters or not. It was also found that the ratio of lattice parameters, $c/a=4.911$, was larger than that of the hexagonal lattice into which the fcc lattice was transformed $2\sqrt{6}=4.899$.

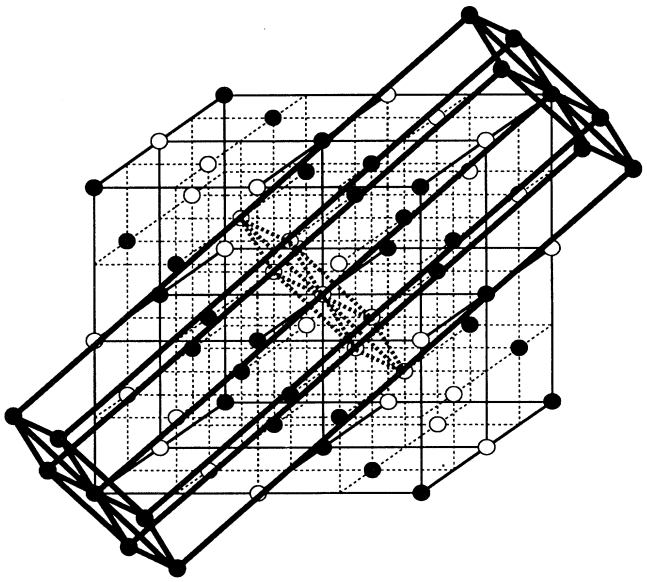

hexagonal lattice; $a=a_0/\sqrt{2}$, $c=2\sqrt{3}a_0$

FIG. 8. The proposed lattice structure of $Zr_{1-x}Sc_xB_{12}$ at low temperatures.

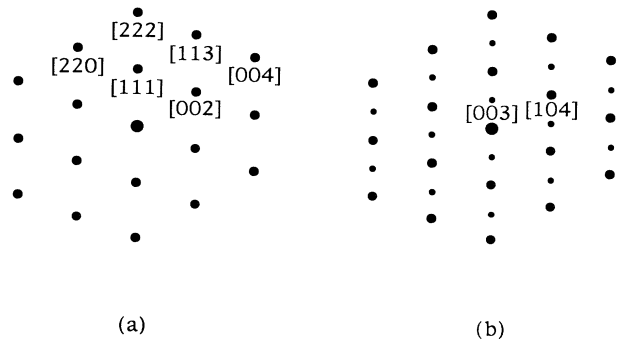

FIG. 9. The schematic drawing of the ED for the high-temperature phase (a) and the low-temperature phase (b) of $Zr_{1-x}Sc_xB_{12}$. The directions of the electron beam are assumed to be [1,1,0] and [0,1,0] and the indices are those for the fcc and the hexagonal lattice, respectively.

TABLE I. The correspondence of the Miller indices of fcc ($h \geq k \geq l \geq 0$) and hexagonal lattices ($h \geq k \geq 0$, $l \geq 0$) in both high- and low-temperature phases. The experimental values of d are those for the sample with $x = 0.3$ at room temperature.

	High-temperature phase		Low-temperature phase	
d (Å)	fcc with $a = a_0$	Hexagonal with $a = a_0/\sqrt{2}$ and $c = \sqrt{3}\ a_0$	fcc with $a = 2a_0$	Hexagonal with $a = a_0/\sqrt{2}$ and $c = 2\sqrt{3}\ a_0$
8.548			(1,1,1)	(0,0,3)
			(3,1,1)	(1,0,1)
4.267	(1,1,1)	(1,0,1),(0,0,3)	(2,2,2)	(1,0,2),(0,0,6)
3.694	(2,0,0)	(1,0,2)	(4,0,0)	(1,0,4)
3.392			(3,3,1)	(1,0,5)
2.850			(3,3,3),(5,1,1)	(0,0,9),(1,0,7)
2.614	(2,2,0)	(1,1,0),(1,0,4)	(4,4,0)	(1,1,0),(1,0,8)
2.500			(5,3,1)	(1,1,3)
			(5,3,3)	(2,0,1)
2.233	(3,1,1)	(2,0,1),(1,1,3),(1,0,5)	(6,2,2)	(2,0,2),(1,1,6),(1,0,10)
2.138	(2,2,2)	(2,0,2),(0,0,6)	(4,4,4)	(2,0,4),(0,0,12)
2.078			(5,5,1),(7,1,1)	(2,0,5),(1,0,11)
1.929			(5,5,3)	(2,0,7),(1,1,9)
1.852	(4,0,0)	(2,0,4)	(8,0,0)	(2,0,8)
1.814			(7,3,3)	(1,0,13)
1.697	(3,3,1)	(2,1,1),(2,0,5),(1,0,7)	(6,6,2)	(2,1,2),(2,0,10),(1,0,14)
1.655	(4,2,0)	(2,1,2),(1,1,6)	(8,4,0)	(2,1,4),(1,1,12)
1.625			(7,5,3),(9,1,1)	(2,1,5),(2,0,11)
1.550			(9,3,1)	(2,1,7)
1.510	(4,2,2)	(3,0,0),(2,1,4),(1,0,8)	(8,4,4)	(3,0,0),(2,1,8),(1,0,16)
			(7,5,5),(7,7,1)	
			(9,3,3)	(3,0,3),(2,0,13)
			(7,7,3),(9,5,1)	(1,1,15),(1,0,17)
	(3,3,3)	(3,0,3),(0,0,9)	(6,6,6)	(3,0,6),(0,0,18)
1.424	(5,1,1)	(2,1,5),(2,0,7)	(10,2,2)	(2,1,10),(2,0,14)
1.380			(9,5,3)	(2,1,11)

B. Origin of phase transition

The plausible origins of the structural transformation as demonstrated in Fig. 8 are (a) a uniform displacement of atoms denoted by closed circles relative to the sites indicated by open circles (model A), (b) the distortion of the B_{12} cubo-octahedra (model B) and (c) diffusion of Zr and Sc atoms (order-disorder transition: model C). It is difficult for model C to explain the temperature dependence of Seebeck coefficient. In fact, the temperature dependence of resistivity for the sample with $x = 0.15$ was unchanged, even when the sample was quenched from room temperature ($> T_c^M$) to liquid He temperature ($\ll T_c^M$). Furthermore, these electric and magnetic properties suggest that the electronic structure was changed drastically when the structural transformation occurred. It is well known that certain electronic phenomena such as nesting of the Fermi surface [charge-density wave (CDW) or spin-density wave] and the Jahn-Teller effect give rise to an electronic phase transition

TABLE II. The results of the refinement of the crystal structure of the low-temperature phase for the sample with $z = 0.4$ in a space group of $R\bar{3}m$. Symbols g and B are the occupation factor and the isotropic thermal parameter, respectively. Figures in parentheses are estimated standard deviations and those without deviations were fixed. $R_{wp} = 12.47\%$, $R_p = 8.58\%$, $R_e = 3.90\%$, $R_I = 4.85\%$, $R_F = 3.84\%$, $a = 0.522\,78(1)$ nm, $c = 2.567\,52(5)$ nm.

Atom	Site	g	x	y	z	B (Å^2)
Zr	c	0.50(2)	0	0	0.2557(2)	0.5
Sc	c	0.50(2)	0	0	0.2557(2)	0.5
B(1)	h	1	0.219(4)	−0.219(4)	0.110(1)	1
B(2)	f	1	0.666(6)	0	0	1
B(3)	h	1	0.220(4)	−0.220(4)	0.608(1)	1
B(4)	g	1	0.664(6)	0	0.5	1

coupled with a structural transformation.

$Zr_{1-x}Sc_xB_{12}$ should have $(2-x)$ valence electrons per metal atom. If only one electron band is filled with these electrons, ZrB_{12} should be insulating. In order to understand the metallic behavior of this compound, we have to consider more than two overlapped bands similar to the case of alkali earth metals. If the Fermi level is located in the overlapped band region, one may expect two types of carriers. Furthermore, if the contribution to the Seebeck coefficient from electrons is larger than that from holes, we can understand the experimental results for ZrB_{12} and the high-temperature phase of $Zr_{1-x}Sc_xB_{12}$. Then with increasing x, the Fermi level should be lowered.

If CDW forms in the electron band at a certain carrier density, the density of state at the Fermi level should be drastically lowered. This kind of the electronic structure may explain the experimental results for the low-temperature phase of $Zr_{1-x}Sc_xB_{12}$. However, it is difficult to understand that the nesting with the wave vector of $\mathbf{Q}=2\pi\mathbf{c}^*$ occurs in the simple band structure of an fcc crystal structure and also that a phase transition of the first-order nature is induced by CDW.

The Jahn-Teller effect is another candidate for the origin of this phase transition. It has been reported that the Jahn-Teller effect is the fundamental reason for general distortions of the B_{12} icosahedral in both molecular and crystal structures.[9] Therefore, it is plausible that the distortion of the B_{12} cubo-octahedra occurred because of the Jahn-Teller effect assuming that the Fermi level was located somewhere in the energy range.

The evidence of a uniform displacement of atoms (model A) was demonstrated by the refinement of the lattice structure in the low-temperature phase. It was difficult by XRD to confirm the existence of the distortion of B_{12} cubo-octahedra (model B). However, it is natural to consider that the B_{12} clusters are distorted, because the distortion of the metallic atoms, which are located interstitial openings among the close-packed B_{12} clusters, has antiferromagneticlike ordering along the c axis of the hexagonal lattice. If such distortion occurred, it should be due to the Jahn-Teller effect. Further investigation of the electronic structure is necessary to understand the details of the phase transition.

The physical properties of the low-temperature phase of $Zr_{1-x}Sc_xB_{12}$ were similar to those of ScB_{12}, but the structure was quite different. Therefore, it is important to investigate the structure of the samples with $x \sim 1$.

V. CONCLUSIONS

We discussed a metal-metal transition in the $Zr_{1-x}Sc_xB_{12}$ system for the composition range of $0.1 \leq x \leq 0.9$. The high-temperature phase was an n-type metal with an fcc structure (so is ZrB_{12}) and the low-temperature phase was a p-type metal (so is ScB_{12}). The structure of the low-temperature phase had a period twice of the high-temperature phase in the direction of (111) and a trigonal space group, $R\bar{3}m$. This structural transformation was thought to be caused by the Jahn-Teller effect based on the deformation of B_{12} cubo-octahedral clusters and followed by the displacement of metallic atoms.

The transition temperature depended on the composition x. Superconductivity occurred for the samples with $x \leq 0.1$ but did not for the sample with $x \geq 0.15$ down to 4.2 K. The latter sample showed a structural transformation. The transition temperature range was wide as a hysteresis was observed. The order parameter which might be proportional to atomic displacement seemed to increase rapidly in this transitional region and get saturated at low temperatures. In order to understand the details of this phase transition, further investigation of the electronic structure is required.

ACKNOWLEDGMENTS

The authors would like to thank Dr. Y. Matsui of the National Institute for Research in Inorganic Materials and Professor S. Uchida of the University of Tokyo for their helpful discussions.

[1]J. G. Bednorz and K. A. Müller, Z. Phys. B **64**, 189 (1986).
[2]R. J. Cava, B. Batlogg, J. J. Krajewski, R. L. Farrow, L. W. Rupp, Jr., A. E. White, K. T. Short, W. F. Peck, Jr., and T. Y. Kometani, Nature (London) **332**, 814 (1988).
[3]A. F. Hebard, M. J. Rosselnsky, R. C. Haddon, D. W. Murphy, S. H. Glarum, T. T. M. Palstra, A. P. Ramlrez, and A. R. Kortan, Nature (London) **350**, 60 (1991).
[4]K. Tanigaki, T. W. Ebbesen, S. Saito, J. Mizuki, J. S. Tsai, Y. Kubo, and S. Kuroshima, Nature (London) **352**, 222 (1991).
[5]B. T. Mattias, T. H. Geballe, K. Andres, E. Corenzwit, G. W. Hull, and J. P. Maita, Science **159**, 530 (1968).
[6]W. N. Lipscomb and D. Britton, J. Chem. Phys. **33**, 275 (1960).
[7]B. Post and F. W. Glaser, J. Metals **4**, 631 (1952).
[8]V. I. Matkovich, J. Economy, R. F. Giese, Jr., and R. B. Barrett, Acta. Crystallogr. **19**, 1056 (1965).
[9]R. Franz and H. Werhcit, Europhys. Lett. **9**, 145 (1985).

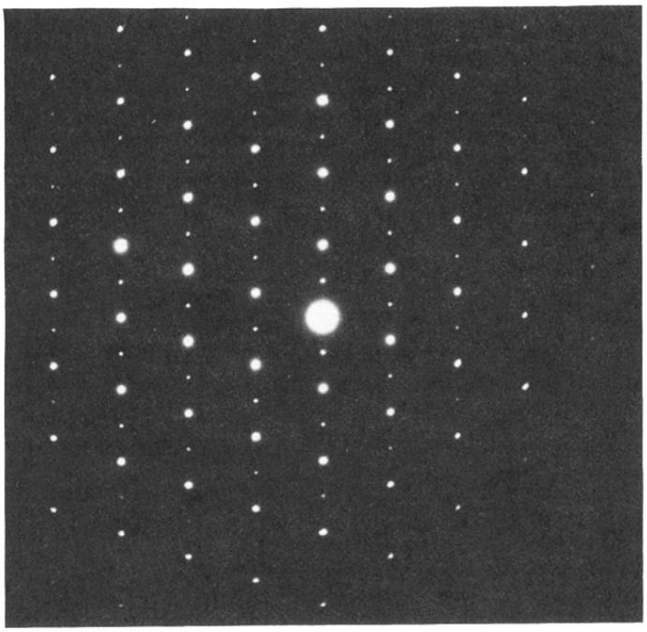

FIG. 6. The electron-diffraction pattern at room temperature for the sample of $Zr_{0.7}Sc_{0.3}B_{12}$.